Prediction of fretting fatigue crack nucleation: comparison between non local fatigue stress analyses

S. Fouvry, B. Berthel

Ecole Centrale de Lyon, LTDS (UMR 5513), Email : siegfried.fouvry@ec-lyon.fr

Abstract

Fretting-Fatigue problems are very complex to address due to the multi-axiality and the very sharp stress gradients imposed below the surface. Multi-axial and non local fatigue approach must be considered. An experimental cylinder/plane fretting fatigue analysis of a 35NiCrMo16 low alloyed steel was performed to investigate the incipient crack nucleation response at 10^6 cycles for various stress gradient conditions. Imposing elastic stress conditions, the Crossland fatigue approach is applied to predict the crack nucleation risk. This analysis confirms that a local stress analysis at the "hot spot" located at surface trailing contact border is not suitable because it sharply overestimates the cracking risk. Non local critical distance and stress gradient approach based on the Papadopoulos theory are applied. The stress gradient formulation provides less dispersive predictions.

Keywords: Fretting Fatigue crack nucleation, Stress gradient, Non local fatigue approach, Crossland, FEM analysis.

1 Introduction

Fretting is a small amplitude oscillatory movement, which may occur between contacting surfaces subjected to vibration or cyclic stress. Combined with cyclic bulk fatigue loading, the so-called fretting-fatigue loading can induce catastrophic cracking phenomena reducing the contact assembly endurances [1, 2]. The crack nucleation phenomenon is commonly addressed by transposing conventional multi-axial fatigue criteria [3] taking into account the stress gradient effects by considering non local fatigue stress analysis [4, 5, 6]. Stress averaging approaches [4, 6], or equivalent critical distance methods [5] which consist in considering the stress state at a "critical distance" from the "hot spot" stress are commonly applied to capture the stress gradient effect. However, these approaches, which consider fixed length scale values are limited when large stress gradient fluctuations are operating [7]. An alternative stress gradient approach which consists in weighting the prediction given at the "hot spot" through a linear decreasing function of the surrounding hydrostatic stress gradient is considered [8, 9]. These two non local fatigue stress analyses are compared regarding well calibrated plain fretting and fretting fatigue crack nucleation experiments.

2 Materials and experimental procedure

2.1 Materials

The studied material is a tempered 35NiCrMo16 low alloyed steel displaying a tempered Martensitic structure. The original austenite grain size is about Ø =10 to 20 µm. The mechanical and fatigue properties of this steel, are summarized in table 1. Chromium 52100 steel was chosen for the cylindrical pads in order to maintain elastically similar conditions whilst simultaneously ensuring that

cracks arose only in 35NiCrMo16 specimens. Both plane and cylindrical pad surfaces were polished to a small Ra=0.05 µm surface roughness.

Table 1. Mechanical and fatigue properties of the studied 35NiCrMo16 low alloyed steel.

E(MPa)	ν	$\sigma_{y0.2\%}$ (MPa)	σ_u (MPa)	σ_d (MPa)	τ_d (MPa)	ΔK_{th} (MPa$\sqrt{m}$)
205000	0.3	950	1130	575	386	3.2

E: Young's modulus; ν: Poisson Coefficient, $\sigma_{y0.2\%}$: Yield stress (0.2%); σ_u: Ultimate Stress; σ_d : traction – compression fatigue limit ($R\sigma=\sigma_{min}/\sigma_{max}$=-1 for 10^7 cycles); τ_d : shear fatigue limit ($R\tau$=-1 for 10^7 cycles); ΔK_{th} : long crack threshold (R=-1).

2.2 Test procedures

Two different test apparatuses were used to quantify respectively the fretting and the fatigue influences in cracking processes. Plain Fretting tests were applied by imposing a nominally static normal force P, followed by an alternated cyclic displacement amplitude (δ*), so that a cyclic tangential load amplitude Q* was generated on the contact surface (Fig. 1a). During a test, P, Q and δ are recorded, from which the δ-Q fretting loop can be plotted. The studied plane specimen is not subjected to any fatigue stress.The fretting fatigue experiments were performed using a dual actuator device [7] (Fig. 1b). This test system allows separate application and control of fretting and fatigue loadings. Like for the plain fretting, the system is instrumented to measure the contact loading (P, Q*, δ*) but also the fatigue stress (σ, $R_\sigma=\sigma_{min}/\sigma_{max}$). Both fretting and fatigue loadings are in phase. All the tests were performed at a constant 13 Hz frequency.

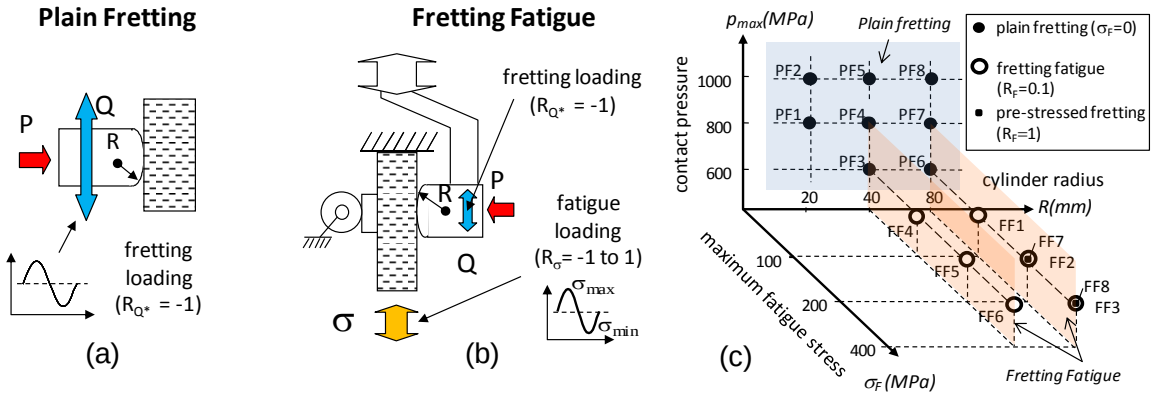

Fig. 1. Schematics of Plain Fretting (a) and Fretting Fatigue (b) experiments; (c) Studied loading conditions.

In order to analyse both contact pressure, fatigue stress and stress gradient effects, various cylinder radii from R= 20 to 80 mm, Hertzian contact pressures from p_{max}=600 to 1000 MPa, fatigue stress conditions from σ_{max}= 0 and 400 MPa and two stress ratios ($R\sigma$=0.1 and 1.0) were investigated (Fig. 1c). The lateral width was adjusted to satisfy Hertzian plain strain hypothesis. Plain fretting tests were first performed to identify the coefficient of friction at the partial slip transition (μ_t=0.8). This value was assumed representative of the friction coefficient operating in the sliding zones of partial slip interfaces. For each R, P and σ loading conditions, an iterative test procedure was applied to identify the threshold tangential force amplitude Q_{CN}* inducing a 10 µm crack length after 10^6 cycles. This crack nucleation investigation was performed applying destructive cross-section expertises. It confirms that crack nucleates systematically on surface at the trailing contact border.

3 Crossland multiaxial fatigue analysis

An analytical stress description was achieved coupling cylinder/plane Mindlin formalism with the McEven stress formulations to extract the stress path below and on the top surface of the studied contacts [7, 10]. The fatigue stress effect on surface shear profile was considered coupling the

Nowell's eccentricity formalism [11]. The major benefits of such analytical formulation are the very fast computation and the exact stress estimation. The fretting stresses imposed below the surface are very complex and therefore a multiaxial fatigue analysis is required. The Crossland's multiaxial fatigue approach [12], well adapted to describe the fatigue response of the studied steel alloy, is considered. The crack risk is expressed as a linear combination of the maximum amplitude of the second invariant of the stress deviator $\sqrt{J_{2,a}}$, and the maximum value of the hydrostatic pressure ($\sigma_{H,max}$) (Fig. 2a). The crack nucleation condition is verified if the maximum equivalent Crossland fatigue stress generated in the contact (i.e. hot spot) becomes larger than the shear fatigue limit :

$$\sigma_C = \sqrt{J_{2,a}} + \alpha_C.\sigma_{H,max} \geq \tau_d \qquad (1)$$

with for the studied alloy $\alpha_C = 0.28$ (Fig. 2a, table 1).

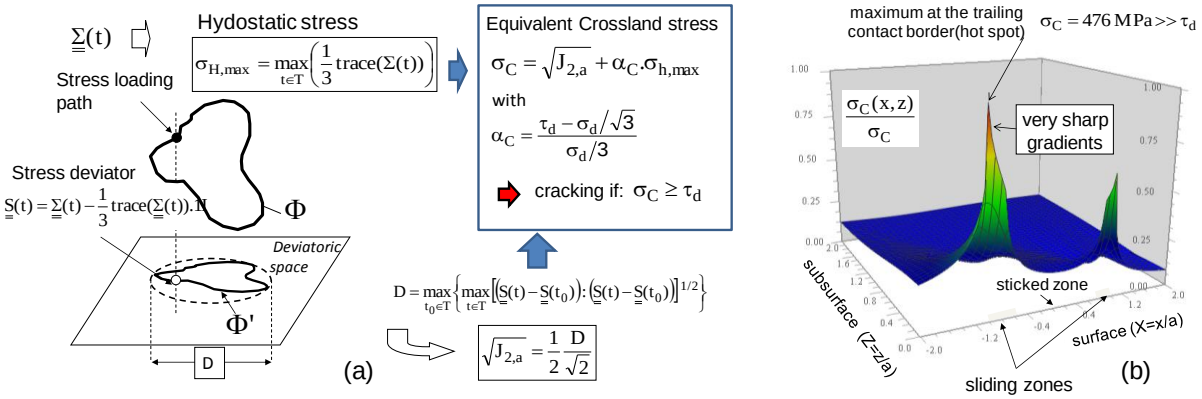

Fig. 2. (a) Illustration of the Crossland criterion – (b) Crossland distribution of the FF2 (Fig.1) condition using an analytical local stress analysis.

Figure 2b displays the Crossland's local stress distribution computed for a representative Fretting Fatigue crack nucleation condition (i.e. FF2, Fig.1). Confirming the expertises, the maximum crack nucleation risk is located at the surface trailing contact border displaying a discontinuous evolution. Indeed very sharp stress gradients are observed as well as a dissymmetry induced by the stick zone eccentricity [11].

4 Results

4.1 "Hot spot" stress analysis

A multi-axial fatigue analysis is first performed using analytical stress computations and a local "hot spot" fatigue stress approach (i.e., trailing contact border stress path). The analysis is performed for each plain fretting and fretting fatigue crack nucleation conditions and reported in a $\sqrt{J_{2,a}}$ - $\sigma_{H,max}$ diagram (Fig. 3). As expected, the experimental data are highly dispersed and systematically above the material boundary. This local Crossland fatigue approach does not integrate the severe stress gradients operating next to the "hot spot" and therefore is not suitable to predict the fretting cracking risk. To quantify the stability of the prediction, the mean value and the square root variance of the equivalent Crossland stress obtained for the 16 test conditions, are computed.

$$\sigma_{C,m} = \frac{1}{N}\sum_{i=1}^{N}\sigma_C(i)\,,\ V\sigma_C = \sqrt{\frac{\sum_{i=1}^{N}\left(\sigma_C(i)-\sigma_{C,m}\right)^2}{N-1}}\,,\ \%E\sigma_C = \left(\frac{\sigma_{C,m}-\tau_d}{\tau_d}\right)x100 \text{ and } \%V\sigma_C = \left(\frac{V\sigma_C}{\tau_d}\right)x100 \qquad (2)$$

The $\%E\sigma_C$ allows to estimate the global error of prediction versus the theoretical material prediction, whereas the $\%V\sigma_C$ variable provides a relative estimation of the dispersion. For the given local fatigue description, we found $\%E\sigma_C$ = +36 % and $\%V\sigma_C$ = 21% which corresponds to a critical overestimation and a high dispersion.

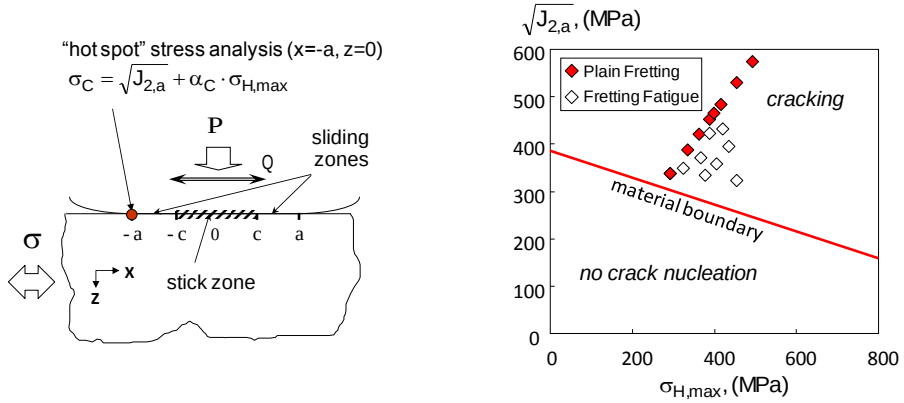

Fig. 3. Local Crossland analysis at the "hot spot" trailing contact border.

4.2 Critical distance

To account for the stress gradient effect, the critical distance approach which consist in considering the stress path at a "ℓ" distance below the "hot spot" trailling contact border for the fatigue analysis is applied [5]. Taylors suggests that optimal critical distance can be related to the half value of the long crack propagation transition b_0 [13]. However better predictions are achieved if the critical distance is defined from the reverse analysis of a reference fretting test solving the following expression :

$$\sigma_C(\ell) = \tau_d \qquad (3)$$

In the present investigation the test condition PF4 (R=40mm, p_{max}=800 MPa) was chosen as the reference test condition to characterize the overall studied stress gradient condition (Fig.1c). Solving equation 3 for $Q^*=Q^*_{CN}$ (PF4) gives $\ell \approx 10\mu m$. This value is then considered to compute the Crossland parameters of the other plain fretting and fretting fatigue crack nucleation conditions. The experimental results are now centered on the material boundary ($\%E\sigma_C(\ell)$= 1%) but the dispersion is still very large ($\%V\sigma_C(\ell)$ = 10%). This suggests that the "critical distance" approach which consider a single "material" length scale parameter is not sufficient to fully capture the stress gradient for such very large stress gradient range.

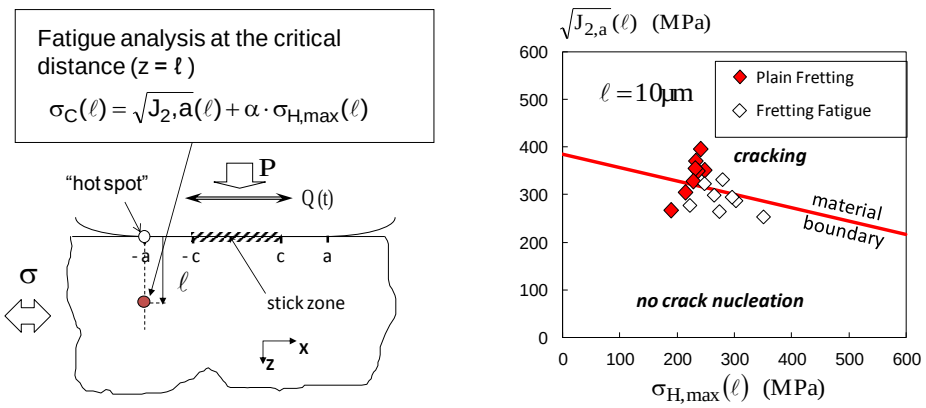

Fig. 4. Critical distance approach assuming a constant length scale value ($\ell = 10\mu m$).

4.3 "stress gradient " approach

An alternative stress gradient strategy consisting in correcting the "hot spot" fatigue stress(σ_C) by a "w" coefficient expressed as a linear decreasing function of the hydrostatic stress gradient operating around the hot spot location is applied [9] (Fig. 4a):

$$\sigma_C^* = \sigma_C \times w \quad \text{where} \quad w = 1 - k.\nabla\sigma_H \tag{3}$$

The hydrostatic stress gradient value is computed applying square area averaging procedure. The chosen edge size is arbitrary fixed equal to the crack nucleation length: $\lambda = b_{CN} = 10\mu m$

For the studied 2D plain strain condition it leads to :

$$\nabla\sigma_H = \sqrt{\left(\frac{\partial\sigma_{H,max}}{\partial x}\right)^2 + \left(\frac{\partial\sigma_{H,max}}{\partial z}\right)^2} \tag{4}$$

so that

$$\nabla\sigma_H = \sqrt{\left(\frac{\sigma_{H,max}(-a,0) - \sigma_{H,max}(-a,\lambda)}{\lambda}\right)^2 + \left(\frac{\sigma_{H,max}(-a,0) - \sigma_{H,max}(-a+\lambda,0)}{\lambda}\right)^2}$$

Where k is the influence factor expressing the reduction of the weight coefficient "w" with the applied stress gradient condition. Indeed, the larger the stress gradient the smaller the "w" weight coefficient multiplied to the "hot spot" stress value. Similar formulations have developed in [14-16].

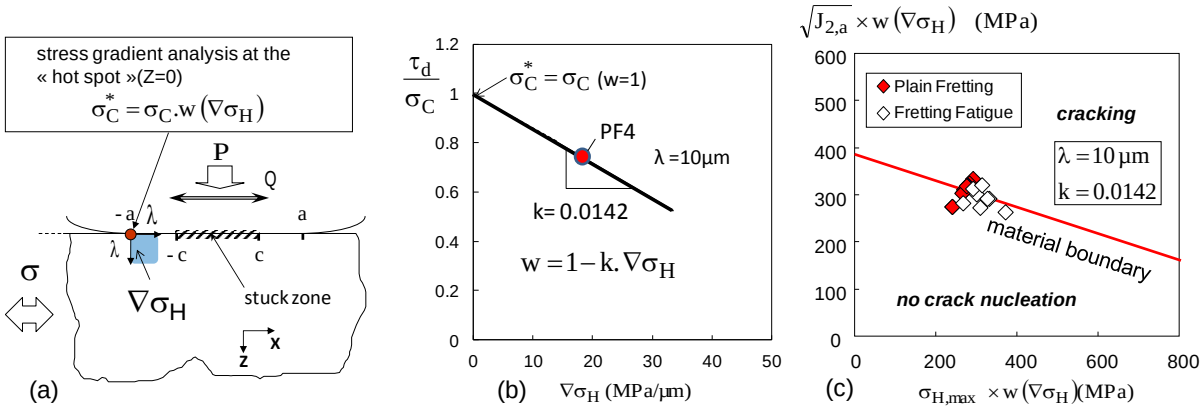

Fig. 5: stress gradient : (a) illustration of the methodology; (b) reverse identification of "k" coefficient from a reference plain fretting test (PF4) (λ =10µm), (c) analysis of experimental results.

A key aspect of this approach is the determination of the "k" factor. The proposed strategy consists in calibrating the linear evolution applying a reverse analysis of the reference (PF4) plain fretting crack nucleation condition. From this test condition we found k =0.0142(MPa/µm)$^{-1}$ (Fig. 5b). Predictions are highly improved (Fig. 5c). All the experimental results are aligned along the material boundary. The statistical analysis leads to $\%E\sigma_C^*$ = 1% and $\%V\sigma_C^*$ = 6%. The prediction is very good, equivalent to the experimental scattering.

5 CONCLUSION

A combined experimental- Crossland modelling approach is developed to rationalize the crack nucleation risk induced by fretting fatigue loadings. It shows that due to the very severe stress gradient imposed by the contact, a local "hot spot" fatigue stress analysis is not suitable. The critical distance method calibrated from a single reference plain fretting test (representative of the medium stress gradient conditions) allows a better averaged prediction but still provides a large discrepancy. The stress gradient approach still calibrated using the single reference plain fretting test displays the best predictions with the lowest scattering. The global comparison of theses different approaches is

illustrated in Figure 6. It can be concluded that the stress gradient approach is better than the usual "critical distance" or equivalent "stress averaging" methods. However it requires the determination of the surface "hot spot" stress which is quite tricky using FEA computations due to convergence aspects. Other strategies based on combined "critical distance – stress gradient" approach [17] or equivalent stress intensity factor description [18-20] can be considered to reduce the mesh size dependency of fretting fatigue crack nucleation predictions.

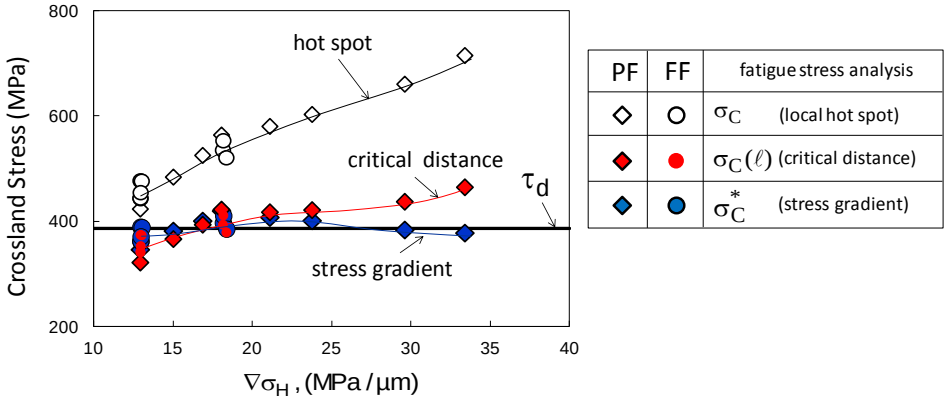

Fig. 6 : Comparison between Crossland stresses computed for the plain fretting (PF) and fretting fatigue (FF) crack nucleation conditions (λ =10µm): the best prediction (i.e. data closer to τ_d fatigue limit) is given by the stress gradient formulation (Eq. 3).

References

[1] R.B. Waterhouse, Fretting Fatigue, Applied Science publishers, 1981.
[2] Y. Mutoh, M. Jayaprakash, Tangential stress range–compressive stress range diagram for fretting fatigue design curve, Tribology International, 44 (2011) 1394–1399,.
[3] M.P. Szolwinski, T.N. Farris, Mechanics of fretting crack formation, Wear, 198, 93-107, 1996.
[4] S. Fouvry, Ph. Kapsa, L. Vincent, A multiaxial fatigue analysis of fretting contact taking into account the size effect, ASTM STP, 1367 (2000) 167-182.
[5] J.A. Araújo, D. Nowell, The effect of rapidly varying contact stress fields on fretting fatigue, Int. J. Fatigue 24(7) (2002) 763-775.
[6] R. Hojjati-Talemi, M. A. Wahab, Fretting fatigue crack initiation lifetime predictor tool: Using damage mechanics approach, Tribology International, 60 (2013) 176-186.
[7] S. Fouvry, H. Gallien, B. Berthel, From uni- to multi-axial fretting-fatigue crack nucleation: Development of a stress-gradient-dependent critical distance approach, Int. J. Fatigue, 62 (2014) 194–209.
[8] I.V. Papadopoulos, V. P. Panoskaltsis, Invariant formulation of a gradient dependant multiaxial high-cycle fatigue criterion, Eng Fract Mech, 55(4) (1996) 513–28.
[9] R. Amargier, S. Fouvry, L. Chambon, C. Schwob, C. Poupon. Stress gradient effect on crack initiation in fretting using a multiaxial fatigue framework, Int J. Fatigue, 32(12) (2010) 1904–1912.
[10] KL. Johnson, Contact Mechanics, Cambridge University Press, 1985.
[11] D. Nowell, D.A. Hills, Mechanics of fretting fatigue tests, Int. J. Mech. Sci., 29(5) (1987) 355-365.
[12] B. Crossland, Proc. of the Inter. Conf. on Fatigue of Metals, Inst. of Mech. Eng., Lond., (1956) 138-149.
[13] D. Taylor, Geometrical effects in fatigue: a unifying theoretical model, Int J Fatigue 22 (1999) 413–420.
[14] Nadot Y, Billaudeau T, Multiaxial fatigue limit criterion for defective materials, Engineering fracture mechanics 73 (2006) 112-133.
[15] F. Morel, A. Morel, Y. Nadot, Comparison between defects and micro-notches in multiaxial fatigue – The size effect and the gradient effect, International Journal of Fatigue, 31 (2009) 263-275.
[16] D.H. Luu, M.H. Maitournam, Q.S. Nguyen, Formulation of gradient multiaxial fatigue criteria, Int. J. Fatigue, 61 (2014) 170–183.
[17] S. Heredia, S. Fouvry, B. Berthel, E. Greco, Introduction of a ''principal stress–weight function'' approach to predict the crack nucleation risk under fretting fatigue, Int. J. Fatigue, 61 (2014) 191–201.
[18] A. Giannakopoulos, T. Lindley, S. Suresh, Aspects of equivalence between contact mechanics and fracture mechanics: theoretical connections and a life-prediction methodology for fretting fatigue, Acta Mater 46 (9) (1998) 2955–2968.
[19] C. Montebello, S. Pommier, K. Demmou, J. Leroux, J. Mériaux, Analysis of stress gradient effect in fretting fatigue trough nonlocal intensity factors, Int J Fatigue 82(0) (2016) 188–198.
[20] S. Fouvry, B. Berthel, Prediction of fretting-fatigue crack nucleation using a surface shear - sliding size crack analog parameter, Procedia Engineering 133 (2015) 179 –191.